This article is published as part of the *Dalton Transactions* themed issue entitled:

Pincers and other hemilabile ligands

Guest Editors Dr Bert Klein Gebbink and Gerard van Koten

Published in issue 35, 2011 of *Dalton Transactions*

Image reproduced with permission of Jun-Fang Gong

Articles in the issue include:

PERSPECTIVE:

ARTICLES:

Dalton Transactions

Dynamic Article Links

Cite this: *Dalton Trans.*, 2011, **40**, 8912

www.rsc.org/dalton

PAPER

Original palladium pincer complexes deriving from 1,3-bis(thiophosphinoyl)indene proligands: C_{sp^3}–H *versus* C_{sp^2}–H bond activation†

Noel Nebra,[a] Jérôme Lisena,[a] Nathalie Saffon,[b] Laurent Maron,*[c] Blanca Martin-Vaca*[a] and Didier Bourissou*[a]

Received 20th January 2011, Accepted 7th March 2011
DOI: 10.1039/c1dt10118h

A series of original 2-indenylidene palladium pincer complexes {PdL[Ind($Ph_2P{=}S)_2$]} (L = $HNCy_2$, PPh_3, Cl^-) have been prepared by double C–H activation of a 1,3-bis(thiophosphinoyl)indene proligand. Crystallographic analyses and DFT calculations indicate that the bonding situation of the {Pd[Ind($Ph_2P{=}S)_2$]} fragment is essentially governed by the conjugated and rigid nature of the dianionic pincer ligand, the nature of the coligand having little influence. The formation of the 2-indenylidene complexes involves either a 2-indenyl pincer or a four-membered cyclometalated complex as an intermediate, suggesting that C_{sp^2}–H or C_{sp^3}–H bond activation takes place. However, deuterium labelling experiences show that in all cases, C_{sp^3}–H bond activation occurs followed eventually by a Pd/H exchange. Nevertheless, evidence for direct C_{sp^2}–H bond activation under mild conditions is obtained when a methyl group is introduced at the indene proligand to prevent C_{sp^3}–H bond activation. The ensuing dissymmetrical 2-indenyl palladium pincer complex has been fully characterized.

Introduction

Cyclometalated pincer complexes were first reported in the middle 1970's by Moulton and Shaw.[1] After a period of latency, they have attracted a surge of interest over the last two decades.[2] In these complexes, the central M–C bond is enforced by the coordination of the peripheral donor groups, and the chelating rigid nature of the ZCZ pincer ligand bestow a unique balance of stability *versus* reactivity. This has led to spectacular catalytic developments especially towards alkane deshydrogenation[3] and alkane metathesis.[4] In addition, the peculiar properties of ZCZ pincer complexes have allowed for the isolation of a variety of highly reactive species relevant to key catalytic transformations.[5–10]

The structure of the ZCZ pincer ligand has been extensively modified in order to finely tune the stereoelectronic properties and thus the reactivity of the ensuing complexes.[11–15] Some representative systems are depicted in Chart 1. Most commonly, the peripheral donor groups are chosen among phosphines, amines, thioethers, thioamides… The central moiety is typically an aryl or an alkyl fragment, so that the great majority of pincer ligands developed thus far are formally monoanionic. A few neutral and

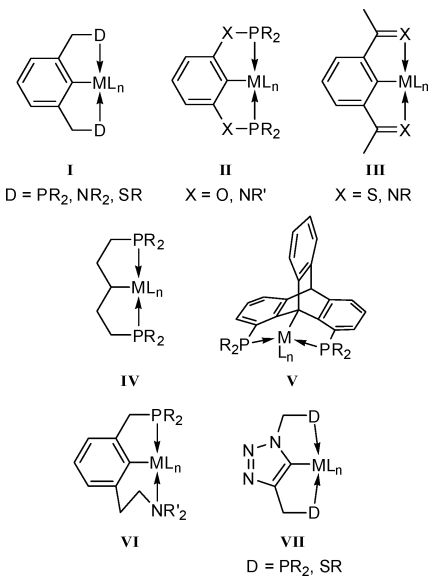

Chart 1 Representative cyclometalated pincer complexes: symmetrical aryl-based complexes **I–III**, symmetrical alkyl-based complexes **IV–V** and dissymmetrical complexes **VI–VII**.

[a]*University of Toulouse, UPS, LHFA, 118 route de Narbonne, F-31062 Toulouse, (France) CNRS, LHFA UMR 5069, F-31062 Toulouse, (France). E-mail: bmv@chimie.ups-tlse.fr, dbouriss@chimie.ups-tlse.fr; Fax: (+33) 5 6155-8204*

[b]*Institut de Chimie de Toulouse, Université Paul Sabatier, FR2599, 118 Route de Narbonne, 31062 Toulouse Cedex 09, (France)*

[c]*University of Toulouse, INSA, UPS, LPCNO, 135 avenue de Rangueil, F-31077 Toulouse, (France) CNRS, LPCNO UMR 5215, F-31077 Toulouse, (France). E-mail: laurent.maron@irsamc.ups-tlse.fr*

† Electronic supplementary information (ESI) available. CCDC reference numbers 800695–800701. For ESI and crystallographic data in CIF or other electronic format see DOI: 10.1039/c1dt10118h

dianionic ZCZ ligands based on *N*-heterocyclic and methanediide skeletons have also been reported.[16] Because of synthetic issues, most of the cyclometalated pincer complexes are symmetrical, but dissymmetrical systems are attracting increasing interest, particularly those displaying hemilabile character.[7,15]

Recently, we have shown that the introduction of coordinating side arms on indene may induce unusual coordination modes.[17] In particular, the presence of two donor buttresses on positions 1 and 3 was found to support the novel 2-indenylidene coordination mode.[17c] Original pincer complexes of Zr and Pd were obtained by double C–H activation of 1,3-bis(thiophosphinoyl)indene and 1,3-bis(phosphazene)indene proligands. Formally, these complexes feature dianionic ZCZ (Z = S, N) pincer ligands. Their bonding situation was analyzed on the basis of crystallographic data and computational studies.[17c] Hereafter, we report a comprehensive study on a series of 2-indenylidene Pd complexes. The coligand in *trans* position to the indenylidene moiety was varied from $NHCy_2$ to Cl^- and PPh_3. A detailed mechanistic study was carried out to gain more insight into the formation of such complexes, and particularly into the underlying C_{sp^3}–H *versus* C_{sp^2}–H bond activation of the 1,3-bis(thiophosphinoyl)indene proligand. A new type of dissymmetrical pincer complex has also been synthesized from a 1-methylated proligand.

Results and discussion

Pincer 2-indenylidene Pd complexes derived from the 1,3-bis(thiophosphinoyl)indene proligand (1-H)

As preliminarily reported,[17c] the $[IndH_2(Ph_2P{=}S)_2]$ proligand **1-H** reacts slowly with $[Pd(cod)Cl_2]$ (cod = cycloocta-1,5-diene) at room temperature in THF. According to NMR spectroscopy this leads to the pincer complex **2**, in which the Pd atom is bonded to C2 (Scheme 1). The addition of two equivalents of Cy_2NH promotes rapid deprotonation of the C_{sp^3}–H bond to afford the novel 2-indenylidene complex **3**, which was characterized by NMR spectroscopy and single-crystal X-ray crystallography. The low solubility of the Pd precursor in typical organic solvents (THF, CH_2Cl_2) probably explains its very slow reaction with **1-H**. With $[Pd(PhCN)_2Cl_2]$, which is much more soluble in organic solvents and whose benzonitrile ligands are more labile than cod, the reaction proceeds much more rapidly and the formation of

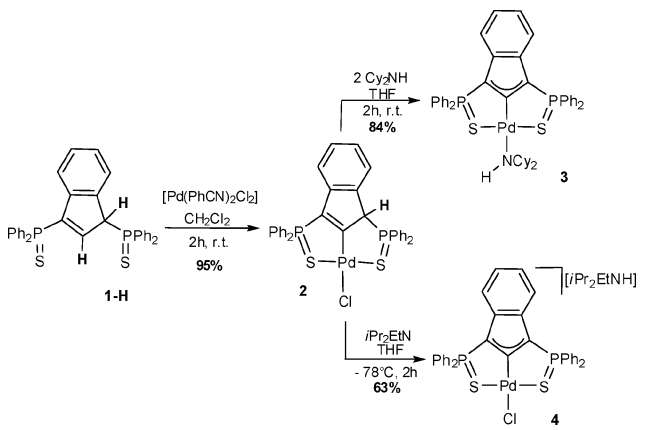

Scheme 1 Preparation of the pincer complexes **2**–**4** from the 1,3-bis(thiophosphinoyl)indene proligand **1-H** and $[Pd(PhCN)_2Cl_2]$.

2 is complete in less than two hours at room temperature in CH_2Cl_2, compared to 10 days using $[Pd(cod)Cl_2]$. Crystals of **2** were obtained from a CH_2Cl_2–Et_2O solution at 20 °C and its structure was definitively confirmed by single-crystal X-ray diffraction study (Fig. 1a). The Pd atom is bonded to the two sulfur atoms, the chlorine atom and C2, which are organized in a quasi-ideal square planar arrangement. The most noticeable geometric difference between **2** and the 2-indenylidene complex **3** is the tetrahedral *versus* planar environment around C1, as the result of the presence, or not, of a residual proton of the proligand. In complex **2**, the C1P1 bond deviates from the mean indenyl plane by 52°, but rotation around this C1P1 bond allows the sulfur atom to be positioned adequately to complete the square planar arrangement around Pd. The dissymmetrical nature of the indenyl in **2** is also apparent from the difference in the C1C2 and C2C3 bond lengths [1.510(5) and 1.353(5) Å, respectively], which are typical for single and double CC bonds, respectively. The Pd–C2 bond length [1.962(4) Å] of **2** is similar to that observed in **3** [1.984(5) Å][17c] and falls in the low range of those reported for palladium $SC_{sp^2}S$ pincer complexes (1.952–2.006 Å).[12c,18]

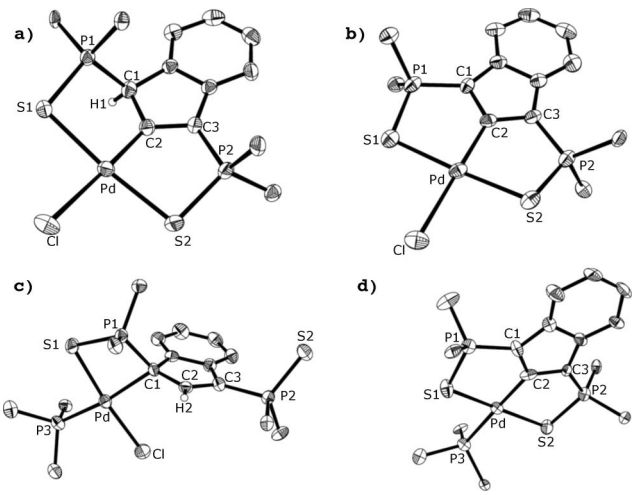

Fig. 1 Ellipsoid drawings (50% probability) of the molecular structures of **2** (a), **4** (b), **5** (c) and **6** (d). For clarity, lattice solvent molecules, hydrogen atoms and the ammonium counter-cation of **4** are omitted and the phenyl groups at phosphorus are simplified.

The preparation of the 2-indenylidene complex featuring a chloride instead of the dicyclohexylamine coligand at Pd was then attempted. Disappointingly, treatment of **2** with one equivalent of Cy_2NH led to an intractable mixture of complexes including **3**. To avoid coordination of the amine to the metal centre, we then turned to diisopropylethylamine (DIEA) instead of Cy_2NH. Monitoring of the reaction between **2** and DIEA by ^{31}P NMR showed the rapid and clean formation of a new symmetrical complex characterized by a singlet signal at δ 43.6 ppm. The signal corresponding to H1 disappeared in the ^1H NMR spectrum, while the ^{13}C NMR spectrum displayed a C_q multiplet signal at δ 163.3 ppm attributed to C2 and an AXX′ system signal at 104.2 ppm attributed to C1 and C3. The similarity between these spectroscopic data and those of **3** strongly argues in favour of the desired 2-indenylidene chloro-palladate complex **4**. Orange crystals suitable for single-crystal X-ray diffraction analysis were obtained from a THF solution at −70 °C, and the structure of

complex **4** was unambiguously confirmed (Fig. 1b). The chloropalladate and ammonium fragments interact *via* a N–H···Cl hydrogen bond [H···Cl distance: 2.35(2) Å and N–H···Cl bond angle: 167.2(7)°].[19] The Pd centre is surrounded by the two sulfur atoms, C2 and the chlorine atom, organized altogether in a square planar arrangement. The Pd–C2 bond length [1.962(7) Å] is very close to those of complexes **2** and **3**. The planar environments around the carbon atoms C1, C2 and C3, combined with the short and almost equal C1C2/C2C3 bond lengths [1.410(9) and 1.435(8) Å] indicate delocalization of the π system, similar to that found in **3** but in contrast to that observed in **2**. Finally, the Pd–Cl bond length [2.4362(18) Å] is substantially longer than that of **2** [2.3807(10) Å] and exceeds those reported for neutral palladium $SC_{sp^2}S$ pincer complexes (2.381–2.407 Å).[12c,18] This feature most likely results from the hydrogen bond with the $(iPr_2EtNH)^+$ counter-cation. Complex **4** is a rare example of an anionic palladium pincer complex stable enough to be structurally characterized.[20,21]

Aiming at further varying the nature of the coligand in the *trans* position to C2, the proligand **1-H** was reacted with a different Pd precursor, namely $[Pd(PPh_3)Cl_2]_2$ (Scheme 2). In this case, no reaction occurred at room temperature in the absence of a base. But when the reaction was carried out in the presence of one equivalent of Cy_2NH, **1-H** was readily converted into a new compound (**5**). The progress of the reaction was easily monitored by ^{31}P NMR spectroscopy: within 1.5 h, the two doublet signals associated with **1-H** (δ 45.5 and 31.3 ppm, J_{PP} = 18.2 Hz) disappeared, while an AMX system appeared. The doublet of doublets at δ 28.3 ppm (J_{PP} = 18.6 and 5.8 Hz) is associated with the PPh_3 coligand, while the two doublet signals at δ 50.4 (J_{PP} = 18.6 Hz) and 33.1 (J_{PP} = 5.8 Hz) ppm are attributed to non-equivalent thiophosphinoyl groups. The latter chemical shifts clearly indicated that only the thiophosphinoyl side arm is coordinated to the Pd atom, in contrast to that observed in complex **2**. The ^1H NMR spectrum of **5** contains no signal attributable to H1 (observed at δ 4.97 ppm for **1-H** and at 5.46 ppm for **2**) but a dd signal at δ 6.49 ppm (J_{HP} = 9.9 and 3.1 Hz) is associated with H2. Consistently, the ^{13}C NMR spectrum displays a C_q ddd signal at δ 30.6 ppm (J_{CP} = 71.5, 62.6, 14.1 Hz) for C1 and a broad unresolved CH signal at δ 148.8 ppm for C2. All these spectroscopic data are consistent with a four-membered metallacyclic structure for complex **5**. This would result from the activation of the C_{sp^3}–H bond, similarly to what had been observed for the reaction of **1-H** and the analogous bisphosphazene derivative $[IndH_2(Ph_2P{=}NMes)_2]$ with $Zr(NMe_2)_4$.[17c]

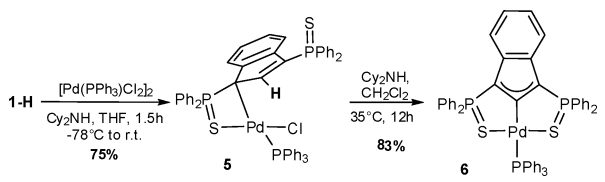

Scheme 2 Preparation of complexes **5** and **6** from the 1,3-bis(thiophosphinoyl)indene proligand **1-H** and $[Pd(PPh_3)Cl_2]_2$.

Crystals of complex **5** were obtained from a CH_2Cl_2–Et_2O solution at room temperature, and its molecular structure was assessed by single-crystal X-ray diffraction (Fig. 1c). The coordination sphere of Pd is composed of Cl, PPh_3, one of the thiophosphinoyl moieties and C1. The overall geometry only slightly deviates from square planar despite the presence of a SPC1Pd four-membered ring [SPC1 bond angle: 81.95(13)°]. The chlorine atom is located in *cis* position to C1,[22] a favourable disposition for further dehydrochlorination and pincer formation (*vide infra*). The cyclometalated carbon atom C1 adopts a distorted tetrahedral environment with the C1–P1 bond deviating from the mean indenyl plane by 41.4°. The Pd–C1 bond length [2.183(5) Å] is significantly longer than those observed in **2** and in **4** [1.962(4) and 1.962(7) Å, respectively] and falls in the typical range of Pd–C_{sp^3} bond lengths.

Treatment of **5** with one equivalent of Cy_2NH or polystyrene supported DIEA (PS-DIEA) in refluxing dichloromethane afforded the corresponding 2-indenylidene complex **6** within 12 h. The A_2X system observed in the ^{31}P NMR spectrum (a doublet at δ 47.0 ppm and a triplet at δ 17.6 ppm, J_{PP} = 50.5 Hz) indicated the coordination of the second thiophosphinoyl side arm and the symmetrisation of the overall structure. ^1H NMR spectroscopy confirmed the removal of H2 and the ^{13}C NMR signal corresponding to C2 appeared as a C_q doublet of triplet at δ 177.8 ppm (J_{PC} = 128.3 and 34.5 Hz). The C1 and C3 atoms are magnetically equivalent and give rise to an AXX′ system at 105.6 ppm, akin to that observed for the 2-indenylidene complexes **3** and **4**. These data are consistent with the coordination of the second thiophosphinoyle group, the shift of the metal centre from C1 to C2, and the concomitant abstraction of a hydrogen atom (see the following section for mechanistic considerations). Fig. 1d shows the solid state structure of **6** as determined by single-crystal X-ray diffraction. It closely resembles those of **3** and **4**, with a square planar arrangement of C2, the two sulfur atoms and PPh_3 around Pd. The Pd–C2 bond length [1.997(9) Å] is similar to those of **3** and **4** [1.984(5) and 1.962(7) Å, respectively]. The carbon atoms C1, C2 and C3 are in planar environments, and π delocalization is apparent from the C1–C2 and C2–C3 bond lengths [1.426(11) and 1.417(11) Å, respectively], which are in between the lengths typically associated with single and double bonds.

The spectroscopic and crystallographic data collected for the three 2-indenylidene complexes complexes **3**, **4** and **6** are very similar, suggesting that the coligand in the *trans* position to C2 has little influence on their structures. To corroborate this observation, DFT calculations were performed on the actual complexes **4** and **6** at the same level of theory as that used previously for complex **3** [B3PW91/SDD(Pd,P),6-31G**(other atoms)].[17c] The optimized structures match nicely those determined experimentally (Table 1), confirming the ability of this computational method to describe such complexes. The bonding situation and especially the nature of the C2–Pd bond was analysed by NBO. As for **3**, a highly covalent σ bond was found between C2 and Pd (65% C2/35% Pd for **4** and 51% C2/49% Pd for **6** compared to 53% C2/47% Pd for **3**) but no π interaction was identified.[17c] The presence of essentially single bonds between C2 and Pd was further confirmed by the corresponding Wiberg indexes (0.73 for **4** and 0.68 for **6**, compared to 0.66 for **3**) (Table 2). In line with the metric data, bond orders significantly higher than 1.0 were found between C1–C2 and C2–C3 (~1.35), consistent with some multiple bond character as the result of π delocalization. The nature of the coligand in *trans* position to C2 influence slightly the atomic charges at Pd and at the elements directly bound to it, but the overall bonding situation

Table 1 Selected geometric data (bond lengths in Å, bond angles in °) for complexes **3**, **4**, **6** and **8** determined experimentally and computed at the B3PW91/SDD(Pd,P),6-31G**(other atoms) level of theory

		S–Pd	C2–Pd	S–P	P–C	S–P–C	$\Sigma C1_\alpha$	$\Sigma C3_\alpha$	$\Sigma C2_\alpha$	C1–C2	C2–C3
3	X-Ray	2.3398(17)	1.984(5)	2.0297(19)	1.719(6)	105.13(19)	359	360	360	1.418(7)	1.425(7)
		2.3360(17)		2.030(2)	1.714(5)	106.39(19)					
	DFT	2.36	1.97	2.07	1.75	106	360	360	360	1.42	1.42
		2.36		2.07	1.75	106					
4	X-Ray	2.3438(19))	1.962(7)	2.021(3)	1.742(7)	106.7(3)	360	360	360	1.435(8)	1.410(9)
		2.3341(19		2.018(3)	1.719(7)	106.9(2)					
	DFT[a]	2.36	1.97	2.06	1.75	107	360	360	360	1.42	1.42
		2.36		2.06	1.75						
6	X-Ray	2.346(2)	1.997(9)	2.033(4)	1.740(8)	105.8(3)	359	359	360	1.417(11)	1.426(11)
		2.319(3)		2.038(4)	1.722(9)	105.3(3)					
	DFT	2.35	2.01	2.07	1.75	106	360	360	360	1.42	1.42
		2.36		2.07	1.75	106					
8	X-Ray	2.3503(16)	1.961(5)	2.015(2)	1.842(5)	104.01(17)	323	360	359	1.520(7)	1.362(7)
		2.3285(16)		2.025(2)	1.772(6)	105.37(18)					
	DFT	2.37	1.96	2.04	1.88	104	323	360	360	1.53	1.37
		2.35		2.06	1.80	105					

[a] The ammonium counter-cation was not included in the calculations.

Table 2 NBO atomic charges and Wiberg indexes for complexes **3**, **4**, **6** and **8**

	NBO Atomic Charges				Wiberg indexes		
	Pd	C2	S	P	C1/C3	Pd–C2	C2–C1/C3
3	0.44	–0.09	–0.55	1.64	–0.66	0.66	1.35
							1.35
4	0.01	–0.05	–0.36	1.60	–0.65	0.73	1.33
							1.33
6	0.33	–0.14	–0.40	1.64	–0.64	0.68	1.34
							1.35
8	–0.002	–0.05	–0.31	1.58	–0.46	0.73	0.98
					–0.54		1.63

Table 3 Crystallographic Data for Compounds **2, 4–8** and **1-Me**

	2	**4**	**5**	**6**	**7**	**1-Me**	**8**
Empirical formula	$C_{34}H_{27}Cl_3P_2PdS_2$	$C_{45}H_{52}ClNOP_2PdS_2$	$C_{52}H_{42}Cl_3P_3PdS_2$	$C_{52}H_{41}Cl_2P_3PdS_2$	$C_{52}H_{42}Cl_2P_3PdS_2,BF_4$	$C_{34}H_{28}P_2S_2$	$C_{35}H_{29}Cl_3P_2PdS_2$
Formula weight	774.37	890.79	1036.64	1000.18	1088.02	562.64	788.39
Crystal system	Monoclinic	Monoclinic	Triclinic	Monoclinic	Triclinic	Monoclinic	Monoclinic
Space group	$P2_1/n$	$P2_1/c$	$P\bar{1}$	$P2_1/c$	$P\bar{1}$	$P2_1/c$	$P2_1/n$
a/Å	10.4520(2)	11.5761(5)	11.4556(3)	8.9679(12)	12.1914(3)	9.3107(2)	9.4787(3)
b/Å	14.1161(3)	24.9932(10)	12.5154(3)	20.433(3)	14.4571(3)	15.8384(3)	33.9812(9)
c/Å	21.7006(5)	14.8809(6)	18.2257(6)	24.908(5)	14.9919(3)	20.4529(4)	10.6863(3)
α/°	90	90	102.868(2)	90	110.963(1)	90	90
β/°	92.020(2)	94.803(3)	96.921(2)	94.220(12)	97.985(1)	106.571(1)	101.622(2)
γ/°	90	90	108.763(2)	90	93.245(2)	90	90
V/Å^3	3199.75(12)	4290.3(3)	2359.21(11)	4551.7(13)	2427.34(9)	2890.85(10)	3371.46(17)
Z	4	4	2	4	2	4	4
Density$_{calcd}$, Mg m^{-3}	1.607	1.379	1.459	1.460	1.489	1.293	1.553
μ/mm^{-1}	1.086	0.701	0.789	0.759	0.729	0.317	1.032
Reflections collected	34 209	41 879	19 928	25 044	36 403	33 762	35 458
Independent reflections	6487	7258	7970	7635	8875	6721	6823
R_1 ($I > 2\sigma(I)$)	0.0407	0.0525	0.0517	0.0702	0.0428	0.0419	0.0513
wR_2	0.0699	0.0986	0.1146	0.0790	0.0857	0.0804	0.0901
(Δ/r)max/e Å^{-3}	0.479 and –0.544	0.595 and –0.850	0.628 and –0.854	0.651 and –0.534	1.096 and –0.809	0.427 and –0.314	0.643 and –0.774
T	173(2)	173(2)	173(2)	173(2)	193(2)	193(2)	193(2)

remains nearly unchanged. Thus, the geometric and electronic properties of the 2-indenylidene complexes **3**, **4** and **6** appear to be governed essentially by the conjugated and rigid nature of the pincer ligand.

Mechanistic investigations of the formation of the pincer complexes: C_{sp^3}–H *versus* C_{sp^2}–H bond activation

From a mechanistic viewpoint, the formation of complexes **2** and **5** from the same proligand **1-H** suggests that either C_{sp^2}–H or C_{sp^3}–H bond activation might take place depending on the nature of the metal precursor, $[Pd(PhCN)_2Cl_2]$ or $[Pd(PPh_3)Cl_2]_2$. In the first case, the presence of two labile nitrile ligands might enable coordination of the two thiophosphinoyl groups of **1-H**, and thereby, the C_{sp^2}–H bond would be ideally positioned to be activated. Since the displacement of PPh_3 is much less favourable than that of PhCN, the reaction of **1-H** with $[Pd(PPh_3)Cl_2]_2$ would rather proceed by coordination of one thiophosphinoyl side arm and activation of the C_{sp^3}–H bond corresponding to the most acidic proton. These two pathways are summarized in Scheme 3.

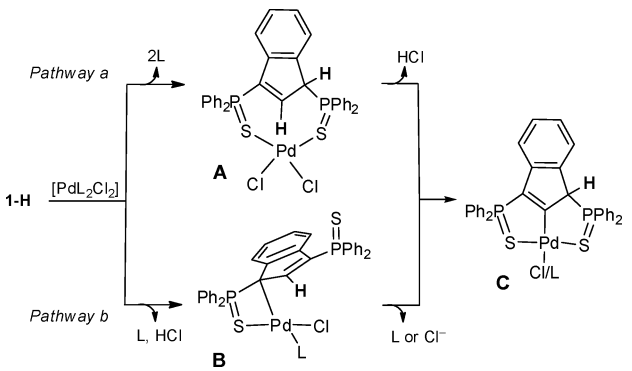

Scheme 3 Plausible pathways for the first C–H bond activation of the indene proligand **1-H** with dichloro palladium precursors.

In order to shed light into the different outcomes observed from the two palladium precursors, the deuterated 1,3-bis(diphenylthiophosphinoyl)indene **1-D** was prepared (Scheme 4). Compound **1-H** was readily deprotonated with *n*BuLi in THF. The ensuing anion $[IndH(Ph_2P{=}S)_2]^-$ is highly stabilized by conjugation, to the extent that it did not react with D_2O. Deuteration was thus achieved with CF_3CO_2D. The absence of the signal characteristic of H1 in the ^1H NMR spectrum of **1-D** unambiguously indicated that the deuterium atom had been

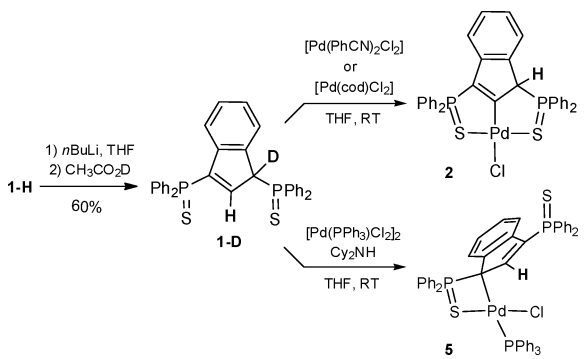

Scheme 4 Preparation of **1-D** and its reactions with $[Pd(PhCN)_2Cl_2]$ and $[Pd(PPh_3)Cl_2]_2$.

introduced in this position. The labelled proligand **1-D** was then reacted with $[Pd(PhCN)_2Cl_2]$ and $[Pd(PPh_3)Cl_2]_2$ under the same conditions as those used with **1-H**. The ensuing complexes **2** and **5** were characterized by ^1H NMR spectroscopy, and both reactions were found to proceed with complete removal of the D-labelling. This result is consistent with the mechanism proposed to account for the formation of **5** (activation of the C_{sp^3}–D bond of **1-D**), but rules out the C_{sp^2}–H bond activation envisioned for **2**. Apparently, the reaction of **1-H/D** with $[Pd(PhCN)_2Cl_2]$ also proceeds *via* activation of the C_{sp^3}–H/D bond. The initially formed four-membered metallacycle **B** would then rearrange by coordination of the second thiophosphinoyl group and concomitant shifts of Pd (from C1 to C2) and H (from C2 to C1).

To provide evidence of such a rearrangement from a four-membered metallacycle of type **B** to a 2-indenyl pincer complex of type **C**, complex **5** was used as a model compound. As mentioned above, the addition of an amine readily converts **5** into the corresponding 2-indenylidene complex **6**. But no intermediate (related to **C**) could be detected by NMR even at low temperature. The thermal activation of **5** in the absence of an amine was also found to afford **6**, but this required temperatures as high as 120 °C and no intermediate could be detected either under these conditions. We thus decided to induce the rearrangement of **5** by creating a vacant site on Pd by chloride abstraction (Scheme 5). The addition of one equivalent of $AgBF_4$ to a CH_2Cl_2 solution of **5** led to a dark red solution. In addition to the signal associated with the PPh_3 coligand (dd, δ 18.9 ppm, J_{PP} = 47.6 and 30.4 Hz), the ^{31}P NMR spectrum of the ensuing complex **7** displayed two dd at δ 54.2 (J_{PP} = 30.4 and 5.3 Hz) and 53.3 ppm (J_{PP} = 47.6 and 5.3 Hz), indicating the coordination of the two thiophosphinoyl side arms in a dissymmetrical manner. In addition, the shift of the proton from C2 to C1 was clearly apparent by ^1H NMR spectroscopy. The corresponding signal resonates at 6.38 ppm in **5** and 5.74 ppm in **7**. These data are consistent with a cationic 2-indenyl pincer structure for **7**. This hypothesis was further corroborated by the formation of the 2-indenylidene complex **6** upon treatment of **7** with Cy_2NH, and definitely confirmed by single-crystal X-ray crystallography (crystals of **7** were obtained by slow diffusion of pentane into a CH_2Cl_2 solution at room temperature). The molecular structure of **7** (Fig. 2) is similar to that of **2**. The most noticeable difference is the slightly longer Pd–C2 bond [2.009(4) Å compared to 1.962(4) Å in **2**], which is probably due to the presence of the triphenylphosphine coligand in the *trans* position to C2.

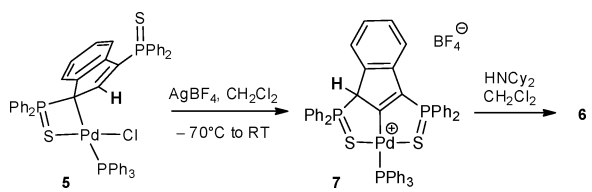

Scheme 5 Pincer formation and Pd/H exchange at C1/C2 upon reaction of complex **5** with a silver salt.

From these mechanistic studies, it can be concluded that the activation of the C_{sp^3}–H bond of **1** is favoured over that of the C_{sp^2}–H bond whatever the palladium precursor. The apparent C_{sp^2}–H bond activation leading to **2** results in fact from the activation of the C_{sp^3}–H bond and subsequent rearrangement. The ability of 1,3-bis(thiophosphinoyl)indene proligands to undergo direct

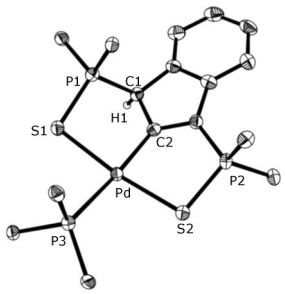

Fig. 2 Ellipsoid drawing (50% probability) of the molecular structure of **7**. For clarity, lattice solvent molecules, hydrogen atoms and the tetrafluoroborate counter-anion are omitted and the phenyl groups at phosphorus are simplified.

C_{sp^2}–H bond activation (Pathway (a) in Scheme 3) thus remains an open question. To address this point, a methyl group was introduced at C1 to obviate the competitive C_{sp^3}–H bond activation, and the preparation of a 2-indenyl pincer complex was envisaged starting from 1-methylindene.

Pincer 2-indenyl Pd complex derived from the 1,3-bis(thiophosphinoyl)-1-methylindene proligand (1-Me)

The 1,3-bis(thiophosphinoyl)-1-methylindene proligand **1-Me** (Scheme 6) was prepared from 1-methylindene, applying a procedure similar to that used for **1-H**. Two consecutive sequences of deprotonation with *n*BuLi followed by addition of chlorodiphenylphosphine, and subsequent oxidation with S_8 afforded **1-Me** in 55% overall yield. Most diagnostic are the ^{1}H NMR signals associated with the methyl group (d, δ 1.75 ppm, J_{PH} = 17.5 Hz) and H2 (dd, δ 6.60 ppm, J_{PH} = 10.1 and 3.1 Hz), as well as the ^{13}C NMR signal corresponding to C1 (dd, δ 58.7 ppm, J_{PC} = 42.7 and 12.3 Hz). The molecular structure of **1-Me**, as assessed by single-crystal X-ray diffraction, is shown in Fig. 3a.

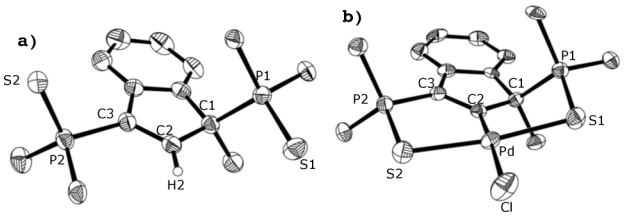

Fig. 3 Ellipsoid drawings (50% probability) of the molecular structures of **1-Me** (a), and **8** (b). For clarity, lattice solvent molecules, hydrogen atoms are omitted and the phenyl groups at phosphorus are simplified.

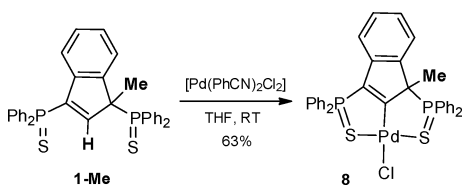

Scheme 6 Preparation of the 2-indenyl pincer complex **8** from the 1,3-bis(thiophosphinoyl)-1-methylindene proligand **1-Me** and $[Pd(PhCN)_2Cl_2]$.

Upon addition to **1-Me** to a THF solution of $[Pd(PhCN)_2Cl_2]$ at room temperature, a light brown solid precipitated instantaneously. ^{31}P NMR spectroscopy indicated the complete consumption of **1-Me** and the formation of a new complex **8** with the two thiophosphinoyl side arms coordinated to Pd (two singlet signals are observed at δ 59.7 and 51.6 ppm). The absence of any ^{1}H NMR signal attributable to H2 suggested that C_{sp^2}–H bond activation had occurred. Consistently, a C_q signal at δ 191.7 ppm was found for C2 in the ^{13}C NMR spectrum. Crystals of **8** were obtained from a CH_2Cl_2–Et_2O solution at room temperature, and its 2-indenyl pincer structure was confirmed by single-crystal X-ray diffraction (Fig. 3b). The Pd centre is surrounded by a chlorine atom, the two thiophosphinoyl side arms and C2 organized in a square-planar arrangement. The metric data of **8** are very close to those of **2**, including the Pd–C2 bond length [1.961(5) Å], the tetrahedral environment around C1 (the C1–P1 bond deviates by 57.7° from the mean indenyl plane) and the pronounced difference in the C1–C2 and C2–C3 bond lengths [1.520(7) and 1.362(7) Å, respectively]. The formation of complex **8** demonstrates that thiophosphinoyl side arms can indeed promote direct C_{sp^2}–H bond activation of indene under mild conditions. This gives access to a new type of pincer complex supported by a dissymmetrical monoanionic ligand.

Finally, DFT calculations were performed to compare the bonding situation in the 2-indenyl complex **8** with that of the 2-indenylidene complexes **3**, **4** and **6**. The geometry determined crystallographically was again nicely reproduced computationally (Table 1). The computed Wiberg indexes are consistent with a single bond character for Pd–C2 and C1–C2 and a double bond character for C2–C3 (Table 2). In addition, NBO analyses revealed noticeable negative atomic charges on C1 and C3 (–0.46 and –0.54, respectively) albeit lower that those found for complexes **3**, **4** and **6**.

Conclusion

From the 1,3-bis(thiophosphinoyl)indene proligand **1-H**, a series of 2-indenylidene palladium pincer complexes have been prepared and characterized by experimental (NMR spectroscopy and single-crystal X-ray diffraction) and theoretical methods. The nature of the coligand in the *trans* position to C2 ($NHCy_2$, Cl^- or PPh_3) was found to have only little influence on the geometric and electronic properties of the complexes that are essentially governed by the conjugated and rigid nature of the pincer ligand. Depending on the palladium precursor used, the 2-indenylidene complex was formed *via* either a 2-indenyl pincer or a four-membered cyclometalated intermediate complex. This suggested that either C_{sp^2}–H or C_{sp^3}–H bond activation took place on **1-H**. However, the deuterium labelling experiences substantiated that in all cases, the coordination of **1-H** involved C_{sp^3}–H bond activation that was eventually followed by concomitant and opposite shifts of Pd and H between C1 and C2. When no competitive C_{sp^3}–H bond activation was possible, the two thiophosphinoyl side arms efficiently promoted direct C_{sp^2}–H bond activation, as evidenced with the 1-methylated indene **1-Me** as proligand. An original dissymmetrical 2-indenyl palladium pincer complex was obtained thereby.

Ongoing studies aim at modulating further the ligand backbone. The reactivity of 2-indenylidene and 2-indenyl pincer complexes is also currently being explored.

Experimental

General comments

All reactions were performed using standard Schlenk techniques under an Argon atmosphere. Solvents were dried and distilled prior to use (Et_2O, THF and toluene over sodium and pentane and dichloromethane over CaH_2). All organic reagents were obtained from commercial sources and used as received. $[Pd(PhCN)_2Cl_2]$ was purchased from STREM. $[Pd(PPh_3)Cl_2]_2$,[23] 1,3-bis(diphenylphosphino)indene[24] and 1,3-bis(diphenylthiophosphinoyl)indene **1-H**[25] were prepared according to literature procedures. ^{31}P, ^{1}H and ^{13}C NMR spectra were recorded on Bruker Avance 300 or 400 and AMX500 spectrometers. ^{31}P, ^{1}H and ^{13}C chemical shifts are expressed with a positive sign, in parts per million, relative to external 85% H_3PO_4 and Me_4Si. Unless otherwise stated, NMR was recorded at 293 K. The ^{1}H and ^{13}C resonance signals were attributed thanks to 2D HMQC and HMBC experiments. The same atom numbering[26] has been used for the indenyl skeleton of all compounds. The N values corresponding to $\frac{1}{2}(J_{AX} + J_{AX'})$ are provided when second order AXX′ systems are observed in the ^{13}C NMR spectra.[27]

Preparations

Synthesis of {PdCl[IndH(Ph$_2$P═S)$_2$]} 2. A colourless solution of **1-H** (1.097 g, 2 mmol) in CH_2Cl_2 (20 mL), was added at room temperature to an orange solution of $[Pd(PhCN)_2Cl_2]$ (768 mg, 2 mmol) in CH_2Cl_2 (20 mL) After stirring for two hours, the solution slightly decoloured and a yellow precipitate appeared. The yellow precipitate was recovered by filtration, washed with CH_2Cl_2 (10 mL) and finally with pentane (2 × 20 mL). After drying under vacuum, **2** was obtained as a pale yellow powder (1.30 g, 95%). NMR data were in agreement with those previously reported.[17c] Single crystals of **2** were grown from a CH_2Cl_2–Et_2O solution at 20 °C.

Synthesis of {PdCl[Ind(Ph$_2$P═S)$_2$]}(*i*Pr$_2$EtNH) 4. iPr$_2$EtN (28 µL, 0.156 mmol) was added to a solution of **2** (107 mg, 0.156 mmol) in THF (30 mL) at −78 °C. After 2 h at this temperature, pentane (40 mL) was added. The resulting precipitate was recovered by filtration and dried under vacuum. Complex **4** was obtained as a yellow solid in good yield (80 mg, 63%). Orange crystals suitable for single-crystal X-ray crystallography were grown from a THF solution at −70 °C. $^{31}P\{^{1}H\}$-NMR (203 K, 121.4 MHz, CD_2Cl_2): δ_{ppm} 43.6 (s). ^{1}H-NMR (203 K, 400 MHz, CD_2Cl_2): δ_{ppm} 7.90 (m, 8H, $H_{ortho}PPh_2$), 7.55–7.40 (m, 12H, $H_{meta,para}PPh_2$) 6.99 (m, 2H, $H_{5,8}$), 6.68 (m, 2H, $H_{6,7}$), 3.54 (m, 2H, NCH_2), 2.95 (m, 2H, NCH), 1.40 (br, 6H, CH_3), 1.29 (br, 3H, CH_3). $^{13}C\{^{1}H\}$-NMR (203 K, 75.5 MHz, CD_2Cl_2): δ_{ppm} 163.3 (m, C_2), 136.4 (m, $C_{4,9}$), 133.4 (d, ^{1}J(C,P) = 81.8 Hz, $C_{ipso}PhP$), 131.8 (m, $C_{meta}PhP$), 128.3 (m, $C_{para,ortho}PhP$), 117.0 (s, $C_{6,7}$), 115.3 (s, $C_{5,8}$), 104.2 (AXX′, N = 73.7 Hz, $C_{1,3}$), 53.6 (s, CH_2), 42.0 (s, CH), 17.8 (s, CH_3), 16.4 (s, CH_3). M. p. 165 °C (dec.).

Synthesis of {Pd(PPh$_3$)Cl[IndH(Ph$_2$P═S)$_2$]} 5. Cy_2NH (40 µl, 0.190 mmol) was added to a suspension of $[Pd(PPh_3)Cl_2]_2$ (86 mg; 0.190 mmol) and **1-H** (104 mg, 0.190 mmol) in THF (30 mL) at −78 °C. After 10 min at this temperature, the reaction was warmed to room temperature and stirred for 1.5 h. The red solution was then filtered to remove the precipitated ammonium salts. Addition of pentane (40 mL) to the red solution resulted in the precipitation of an orange–red solid. The solvent was filtered off and the orange solid was dried under vacuum to yield **5** (140 mg, 75% yield). Single crystals were grown from a CH_2Cl_2–Et_2O solution at 20 °C. $^{31}P\{^{1}H\}$-NMR (121.4 MHz, $CDCl_3$): δ_{ppm} 50.4 (d, ^{3}J(P,P) = 18.6 Hz, P_1), 33.1 (d, ^{5}J(P,P) = 5.8 Hz, P_2), 28.3 (dd, ^{3}J(P,P) = 18.6 Hz, ^{5}J(P,P) = 5.8 Hz, PPh_3). ^{1}H-NMR (500.3 MHz, $CDCl_3$): δ_{ppm} 8.38–8.32 (m, 2H, $H_{ortho}PhP$), 7.99–7.93 (m, 5H, PPh and $H_{5\ or\ 8}$), 7.75–7.23 (m, 30H, PPh and $H_{5\ or\ 8}$), 7.05 (m, 2H, $H_{6,7}$), 6.49 (dd, 1H, ^{3}J(H,P) = 9.1 Hz, ^{3}J(H,P) = 3.3 Hz, 1H, H_2). $^{13}C\{^{1}H\}$-NMR (100.6 MHz, $CDCl_3$): δ_{ppm} 147.1 (m, C_2), 144.5 (m, C_9), 141.6 (ddd, ^{2}J(C,P) = 12.9 Hz, ^{3}J(C,P) = 9.9 Hz and ^{4}J(C,P) = 0.8 Hz, C_4), 135.1–127.9 (Ph_2P and Ph_3P), 127.1 (dd, ^{1}J(C,P) = 12.0 Hz and ^{3}J(C,P) = 6.2 Hz, C_3), 123.8 (s, C_{Ind}), 123.5 (s, C_{Ind}), 123.1 (s, C_{Ind}), 30.6 (ddd, ^{1}J(CP) = 71.5 Hz, ^{2}J(C,P) = 62.6 Hz and ^{3}J(C,P) = 14.1 Hz, C_1). Elemental analysis calcd (%) for $C_{51}H_{40}ClP_3PdS_2$: C 64.36, H 4.24; found C 64.16, H 4.29. M. p. 192–193 °C.

Synthesis of {Pd(PPh$_3$)[Ind(Ph$_2$P═S)$_2$]} 6. Compound **5** (210 mg, 0.230 mmol) and polystyrene supported diisopropylethylamine (PS-DIEA, 0.330 mg, 4 equiv.) were heated in CH_2Cl_2 (20 mL) at 35 °C during 12 h. Total consumption of compound **5** was confirmed by ^{31}P NMR spectroscopy. The deep-orange solution was then filtered to remove the PS-DIEA ammonium salts. The solution was concentrated under vacuum and an orange solid was precipitated by addition of pentane (40 mL). Filtration and vacuum drying yielded an orange solid (175 mg, 83% yield). Single crystals of **6** were grown from a CH_2Cl_2–Et_2O solution at 20 °C. $^{31}P\{^{1}H\}$-NMR (121.4 MHz, $CDCl_3$): δ_{ppm} 47.0 (d, ^{3}J(P,P) = 50.5 Hz, P═S), 17.6 (t, ^{3}J(P,P) = 50.5 Hz, PPh_3). ^{1}H-NMR (500.3 MHz, C_6D_6): δ_{ppm} 7.84 (m, 8H, $H_{meta}Ph_2P$), 7.67 (m, 6H, $H_{meta}PPh_3$), 7.50–7.30 (m, 15H, $H_{ortho,para}$ Ph_2P and PPh_3), 7.18 (m, 2H, $H_{6,7}$), 6.83 (m, 2H, $H_{5,8}$). $^{13}C\{^{1}H\}$-NMR (125.8 MHz, C_6D_6): δ_{ppm} 177.8 (dt, ^{2}J(C,P) = 128.3 and 34.5 Hz, C_2), 137.9 (m, $C_{4,9}$), 134.6 (d, ^{3}J(C,P) = 12.6 Hz, $C_{ortho}Ph_3P$), 132.8 (d, ^{1}J(C,P) = 82.1 Hz, $C_{ipso}PhP$), 132.2 (d, ^{2}J(C,P) = 11.7 Hz, $C_{ortho}PhP$), 131.3 (m, $C_{para}PhP$), 130.0 (m, $C_{para}PhP$), 129.08 (m, $C_{meta}PhP$), 128.17 (m, $C_{para}PhP$), 117.60 (s, $C_{5,8}$), 116.9 (s, $C_{6,7}$), 105.6 (AXX′, N = 76.1 Hz, $C_{1,3}$). Elemental analysis calcd (%) for $C_{51}H_{39}P_3PdS_2$: C 66.92, H 4.29; found: C 66.62, H 4.10. M.p. 234–236 °C (dec.).

Synthesis of [IndHD(Ph$_2$P═S)$_2$]. *n*Buli (230 µL, 1,6 M in hexane) was added to a degassed solution of $[IndH_2(P{=}S)_2]$ (201 mg, 0,366 mmol) in THF (20 mL) at −80 °C. The mixture was stirred for 30 min and then the reaction mixture was warmed slowly to room temperature under stirring. CF_3COOD was then added (30 µL) at −80 °C. After warming up to room temperature, the THF was partially eliminated under vacuum, and a white precipitate appeared. The deuterated ligand was then recovered by filtration and dried under vacuum. The product is moisture sensitive (lost of D-labelling), and was stored in glove box. Yield 122 mg (60%). $^{31}P\{^{1}H\}$ NMR (121.4 MHz, $CDCl_3$): δ_{ppm} 45.5 (d, ^{4}J(P,P) = 3.7 Hz, P_1), 30.4 (d, ^{4}J(P,P) = 4.2 Hz, P_2). ^{1}H NMR (300 MHz, $CDCl_3$): δ_{ppm} 7.73–6.77 (m, 24H, H_{5-8} and PPh_2), 6.36 (ddd, ^{3}J(P,H) = 10.1 Hz, ^{3}J(P,H) = 3.9 Hz, ^{3}J(H,H) = 0.9 Hz, 1H, H_2), 4.90 (d br, ^{2}J(P,H) = 22.0 Hz, 1H, H_1).

Synthesis of {Pd(PPh$_3$)[IndH(Ph$_2$P═S)$_2$]}[BF$_4$] 7. To a solution of **5** (50.5 mg, 0.053 mmol) in CH_2Cl_2 (3 mL) at −80 °C was

added a suspension of $AgBF_4$ in CH_2Cl_2 (1 mL). The solution was stirred at −80 °C for 1 h. and then warmed to room temperature. The deep-orange solution was then filtered to remove the silver salts. The solution was concentrated under vacuum and pentane (4 mL) was added. Filtration and vacuum drying yielded an orange solid. Crystals suitable for single-crystal X-ray crystallography were obtained by slow diffusion of pentane into CH_2Cl_2 at room temperature. Yield 21 mg (40%). $^{31}P\{^1H\}$ NMR (121.4 MHz, $CDCl_3$): δ_{ppm} 54.2 (dd, $^3J(P,P) = 30.4$ Hz, $^4J(P,P) = 5.3$ Hz, P_1), 53.3 (dd, $^3J(P,P) = 47.6$ Hz, $^4J(P,P) = 5.3$ Hz, P_2), 18.9 (dd, $^3J(P,P) = 47.7$ Hz, $^3J(P,P) = 30.4$ Hz, PPh_3). ^1H NMR (500 MHz, $CDCl_3$): δ_{ppm} 7.84–7.75 (m, 4H, PhP), 7.71–7.67 (m, 2H, PhP), 7.64–7.59 (m, 8H, PhP), 7.55 (m, 5H, PhP), 7.52 (m, 2H, Ph), 7.46 (m, 6H, Ph), 7.42–7.38 (m, 2H, Ph), 7.33 (m, 1H, H_6), 7.27–7.20 (m, 2H, $H_{5,7}$), 7.13–7.08 (m, 3H, Ph), 7.01–6.98 (m, 4H, Ph), 6.73 (d, $^3J(H,H) = 7.5$ Hz, 1H, H_8), 5.74 (dd, $^2J(H,P) = 24.8$ Hz, $^4J(H,P) = 2.7$ Hz, 1H, H_1). ^{13}C NMR (125 MHz, $CDCl_3$): δ_{ppm} 190.6 (ddd, $^2J(P,C) = 7.1$ Hz, $^2J(P,C) = 32.2$ Hz, $^2J(P,C) = 135.9$ Hz, C_2), 147.5 (dd, $^1J(P,C) = 104.7$ Hz, $^3J(P,C) = 10.0$ Hz, C_3), 145.1 (ddd, $^4J(P,C) = 3.1$ Hz, $^3J(P,C) = 6.5$ Hz, $^2J(P,C) = 19.8$ Hz, C_4), 140.2 (m, C_9), 134.8–119.7 (m, Ph_2P), 133.9 (d, $^2J(P,C) = 12.2$ Hz, $C_{ortho}PPh_3$), 131.3 (m, $C_{para}PPh_3$), 130.1 (d, $^1J(P,C) = 49.1$ Hz, $C_{ipso}Ph_3P$), 129.6 (s, C_5), 129.0 (d, $^3J(P,C) = 10.2$ Hz, $C_{meta}PPh_3$), 125.9 (s, C_7), 126.4 (d, $^1J(P,C) = 80.2$ Hz, $C_{ipso}PhP$), 126.3 (d, $^1J(P,C) = 84.7$ Hz, $C_{ipso}PhP$), 125.0 (d, $^1J(P,C) = 76.3$ Hz, $C_{ipso}PhP$), 123.8 (s, C_6), 119.8 (s, C_8), 119.7 (d, $^1J(P,C) = 82.4$ Hz, $C_{ipso}PhP$), 71.1 (ddd, $^1J(P,C) = 51.9$ Hz, $^3J(P,C) = 20.2$ Hz, $^3J(P,C) = 3.1$ Hz, C_1). M. p. 186–188 °C.

Synthesis of [IndH(Me)(Ph$_2$P═S)$_2$] 1-Me. To a solution of 1-methylindene (3.36 g, 25.8 mmol) in diethyl ether (50 mL) was added dropwise *n*BuLi (16.13 mL of a 1.6 M hexane solution, 25.8 mmol) at −80 °C. The mixture was stirred at −80 °C for 1 h and then warmed slowly to room temperature. The solution was cooled again to −80 °C and diphenylchlorophosphine (4.77 mL, 25.8 mmol) was added. The reaction medium was stirred at −80 °C for 30 min and then warmed to room temperature within 1 h. The addition of *n*BuLi and diphenylchlorophosphine was repeated under the same conditions. S_8 (1.65 g, 51.6 mmol of S) was then added to the formed solution of 1,3-bis(diphenylphosphino)-1-methylindene. The mixture was stirred for 10 h, the solvent was removed by filtration and toluene (80 mL) was added. The whitish precipitate was recovered by filtration and washed with toluene and pentane. The Ind(Me)(P═S)$_2$ is obtained as a white powder (7.89 g, 14.02 mmol, 55%). Crystals suitable for single-crystal X-ray crystallography were obtained from a CH_2Cl_2 solution at room temperature. $^{31}P\{^1H\}$ NMR (121.4 MHz, $CDCl_3$): δ_{ppm} 53.8 (d, $^4J(P,P) = 4.4$ Hz, P_1), 31.2 (d, $^4J(P,P) = 4.4$ Hz, P_2). ^1H NMR (300 MHz, $CDCl_3$): δ_{ppm} 7.73–7.67 (m, 4H, PhP), 7.63–7.56 (m, 4H, PhP), 7.53–7.46 (m, 4H, PhP), 7.45–7.39 (m, 4H, H_5 and PhP), 7.36 (m, 5H, H_7 and PhP), 7.32–7.26 (m, 1H, PhP), 7.22–7.19 (m, 2H, $H_{8,6}$), 6.60 (dd, $^3J(P,H) = 10.1$ Hz, $^3J(P,H) = 3.1$ Hz, 1H, H_2), 1.75 (d, $^3J(P,H) = 17.5$ Hz, 3H, H_{10}). ^{13}C NMR (75 MHz, $CDCl_3$): δ_{ppm} 151.6 (dd, $^2J(P,C) = 8.9$ Hz, $^2J(P,C) = 1.4$ Hz, C_2), 146.5 (dd, $^2J(P,C) = 9.5$ Hz, $^3J(P,C) = 0.4$ Hz, C_9), 141.6 (dd, $^2J(P,C) = 12.4$ Hz, $^3J(P,C) = 3.6$ Hz, C_4), 138.7 (dd, $^1J(P,C) = 84.8$ Hz, $^3J(P,C) = 8.5$ Hz, C_3), 133.3 (d, $^2J(P,C) = 9.4$ Hz, $C_{ortho}PhP$), 132.2 (d, $^2J(P,C) = 9.5$ Hz, $C_{ortho}PhP$), 132.0 (d, $^4J(P,C) = 2.9$ Hz, $C_{para}PhP$), 131.9 (d, $^4J(P,C) = 3.1$ Hz, $C_{para}PhP$), 131.9 (d, $^2J(P,C) = 11.2$ Hz, $C_{ortho}PhP$), 131.7 (d, $^4J(P,C) = 3.0$ Hz, $C_{para}PhP$), 131.6 (d, $^1J(P,C) = 86.8$ Hz, $C_{ipso}PhP$), 131.6 (d, $^2J(P,C) = 11.6$ Hz, $C_{ortho}PhP$), 130.8 (d, $^1J(P,C) = 86.5$ Hz, $C_{ipso}PhP$), 130.7 (d, $^1J(P,C) = 78.8$ Hz, $C_{ipso}PhP$), 128.7 (d, $^3J(P,C) = 2.4$ Hz, $C_{meta}PhP$), 128.6 (d, $^3J(P,C) = 2.4$ Hz, $C_{meta}PhP$), 128.3 (d, $^1J(P,C) = 77.4$ Hz, $C_{ipso}PhP$), 128.3 (d, $^3J(P,C) = 2.3$ Hz, $C_{meta}PhP$), 128.2 (d, $^3J(P,C) = 1.9$ Hz, $C_{meta}PhP$ and C_6), 126.4 (d, $^3J(P,C) = 1.3$ Hz, C_8), 124.7 (d, $^3J(P,C) = 1.9$ Hz, C_5), 123.9 (s, C_7), 58.7 (dd, $^1J(P,C) = 42.7$ Hz, $^3J(P,C) = 12.3$ Hz, C_1), 19.2 (s, C_{10}). M.p. 185 °C (dec.). Elemental analysis calcd (%) for $C_{34}H_{28}P_2S_2$: C 72.58, H 5.02; found: C 72.80, H 4.86. HRMS (TOF, CI+): calculated for $C_{34}H_{29}P_2S_2$: 563.1186, found: 563.1172.

Synthesis of {PdCl[Ind(Me)(Ph$_2$P═S)$_2$]} 8. A solution of **1-Me** (250 mg, 0.444 mmol) in THF (10 mL) was added to a stirred solution of $[Pd(PhCN)_2Cl_2]$ (170 mg, 0.444 mmol) in THF (5 mL) at room temperature. A brown precipitate appeared immediately. The mixture was stirred for 2 h. to ensure complete reaction. The precipitate was recovered by filtration and washed with THF (5 mL). After extraction with CH_2Cl_2 and drying under vacuum, complex **8** was obtained as a brown precipitate (196 mg, 63% yield). Crystals suitable for single-crystal X-ray analysis were obtained by slow diffusion of Et_2O into a CH_2Cl_2 solution at room temperature. $^{31}P\{^1H\}$ NMR (121.4 MHz, $CDCl_3$): δ_{ppm} 59.7 (s, P_1), 51.6 (s, P_2). ^1H NMR (300 MHz, $CDCl_3$): δ_{ppm} 8.02–7.95 (m, 2H, $H_{ortho}PhP$), 7.75–7.67 (m, 3H, PhP), 7.65–7.51 (m, 4H, PhP), 7.50–7.40 (m, 5H, PhP and H_5), 7.32–7.27 (m, 4H, PhP and $H_{6,7}$), 7.21–7.08 (m, 5H, PhP), 6.73 (m, 1H, H_8), 1.93 (d, $^3J(P,H) = 18.4$ Hz, 3H, H_{10}). ^{13}C NMR (125 MHz, $CDCl_3$): δ_{ppm} 191.7 (m, C_2), 146.5 (d, $^2J(P,C) = 9.1$ Hz, C_9), 144.2 (dd, $^2J(P,C) = 18.4$ Hz, $^3J(P,C) = 3.7$ Hz, C_4), 143.2 (dd, $^1J(P,C) = 107.1$ Hz, $^3J(P,C) = 9.3$ Hz, C_3), 133.6 (d, $^4J(P,C) = 2.3$ Hz, $C_{para}PhP$), 133.3 (d, $J(P,C) = 9.7$ Hz, $C_{ortho/meta}PhP$), 133.1 (d, $^4J(P,C) = 3.4$ Hz, $C_{para}PhP$), 133.1 (d, $J(P,C) = 9.3$ Hz, $C_{ortho/meta}PhP$), 132.7 (d, $^4J(P,C) = 2.7$ Hz, $C_{para}PhP$), 136.5 (d, $J(P,C) = 11.2$ Hz, $C_{ortho/meta}PhP$), 132.4 (d, $^4J(P,C) = 4.7$ Hz, $C_{para}PhP$), 131.8 (d, $J(P,C) = 11.5$ Hz, $C_{ortho/meta}PhP$), 129.2 (d, $J(P,C) = 13.5$ Hz, $C_{ortho/meta}PhP$), 129.1 (d, $J(P,C) = 13.1$ Hz, $C_{ortho/meta}PhP$), 128.7 (s, C_5), 128.2 (d, $J(P,C) = 12.4$ Hz, $C_{ortho/meta}PhP$), 128.1 (d, $^1J(P,C) = 84.3$ Hz, $C_{ipso}PhP$), 128.0 (d, $^1J(P,C) = 80.6$ Hz, $C_{ipso}PhP$), 124.6 (d, $^1J(P,C) = 69.2$ Hz, $C_{ipso}PhP$), 124.5 (s, C_7), 122.8 (s, C_6), 118.9 (s, C_8), 75.3 (dd, $^1J(P,C) = 59.0$ Hz, $^3J(P,C) = 17.7$ Hz, C_1), 21.3 (d, $^3J(P,C) = 18.3$ Hz, C_{10}). HRMS (TOF, CI+): calculated for $C_{34}H_{27}ClP_2PdS_2$: 703.9752, found: 703.9746. M.p. 280 °C (dec.).

Crystal Structure Determination of complexes 2, 4, 5, 6, 7, 1-Me and 8

Data were collected using an oil-coated shock-cooled crystal on a Bruker-AXS SMART APEX II diffractometer with Mo-Kα radiation ($\lambda = 0.7103$ Å). Semi-empirical absorption corrections were employed.[28] The structures were solved by direct methods (SHELXS-97)[29] and refined using the least-squares method on F^2.[30] For compounds **2**, **4** and **6**, restraints were used to refine disorders. The similar-ADP (Anisotrope Displacement Parameter) and rigid-bond restraints were employed to make the ADP values of the disordered atoms more reasonable.

CCDC 800695 (**2**), 800696 (**4**), 800697 (**5**), 800698 (**6**), 800699 (**7**), 800700 (**1-Me**) and 800701 (**8**) contain the supplementary crystallographic data for this paper.† The crystallographic data for the structures is given in Table 3.

Computational details

Palladium and Phosphorus were treated with a Stuttgart–Dresden pseudopotential in combination with their adapted basis set.[31,32] In all cases, the basis set has been augmented by a set of polarization function (f for Pd and d for P).[33] Carbon, sulfur, nitrogen and hydrogen atoms have been described with a 6-31G(d,p) double-ζ basis set.[34] Calculations were carried out at the DFT level of theory using the hybrid functional B3PW91.[35,36] Geometry optimisations were carried out without any symmetry restrictions, the nature of the *extrema* (*minimum*) was verified with analytical frequency calculations. All these computations have been performed with the Gaussian 98[37] suite of programs. The bonding situation was analyzed using the NBO technique.[38]

Acknowledgements

We are grateful to the CNRS, UPS, ANR program (ANR-06-BLAN-0034) and COST action CM0802 (PhoSciNet) for financial support of this work. CalMip (CNRS, Toulouse, France) is acknowledged for calculation facilities. The Institut Universitaire de France (L. M.), the Spanish MEC and the European Social Fund (N. N. post-doctoral grant) and French MESR (J. L. PhD grant) are kindly acknowledged for financial support.

Notes and references

1 C. J. Moulton and B. L. Shaw, *J. Chem. Soc., Dalton Trans.*, 1976, 1020.
2 (*a*) M. E. Van der Boom and D. Milstein, *Chem. Rev.*, 2003, **103**, 1759; (*b*) *The Chemistry of Pincer Ligands*, D. Morales-Morales and C. M. Jensen, Ed., Elsevier, Oxford , 2007; (*c*) D. Benito-Garagorri and K. Kirchner, *Acc. Chem. Res.*, 2008, **41**, 201.
3 (*a*) M. Gupta, C. Hagen, W. C. Kaska, R. E. Cramer and C. M. Jensen, *J. Am. Chem. Soc.*, 1997, **119**, 840; (*b*) F. Liu, E. B. Pak, B. Singh, C. M. Jensen and A. S. Goldman, *J. Am. Chem. Soc.*, 1999, **121**, 4086; (*c*) K. Krogh-Jespersen, M. Czerw, K. Zhu, B. Singh, M. Kanzelberger, N. Darji, P. D. Achord, K. B. Renkema and A. S. Goldman, *J. Am. Chem. Soc.*, 2002, **124**, 10797; (*d*) K. Zhu, P. D. Achord, X. Zhang, K. Krogh-Jespersen and A. S. Goldman, *J. Am. Chem. Soc.*, 2004, **126**, 13044; (*e*) I. Göttker-Schnetmann, P. White and M. Brookhart, *J. Am. Chem. Soc.*, 2004, **126**, 1804; (*f*) I. Göttker-Schnetmann and M. Brookhart, *J. Am. Chem. Soc.*, 2004, **126**, 9330.
4 (*a*) A. S. Goldman, A. H. Roy, Z. Huang, R. Ahuja, W. Schinski and M. Brookhart, *Science*, 2006, **312**, 257; (*b*) R. Ahuja, S. Kundu, A. S. Goldman, M. Brookhart, B. C. Vicente and S. L. Scott, *Chem. Commun.*, 2008, 253.
5 M. Albrecht, A. L. Spek and G. van Koten, *J. Am. Chem. Soc.*, 2001, **123**, 7233.
6 For an amido hydride complex of iridium, see: J. Zhao, A. S. Goldman and J. F. Hartwig, *Science*, 2005, **307**, 1080.
7 For a Pt(IV) oxo complex, see: (*a*) E. Poverenov, I. Efremenko, A. I. Frenkel, Y. Ben-David, D. J. W. Shimon, G. Leitus, L. Konstantinovski, J. M. L. Martin and D. Milstein, *Nature*, 2008, **455**, 1093; (*b*) C. Limberg, *Angew. Chem. Int. Ed.*, 2009, **48**, 2270.
8 For iridium dioxygen complexes, see: D. B. Williams, W. Kaminsky, J. M. Mayer and K. I. Goldberg, *Chem. Commun.*, 2008, 4195.
9 For palladium hydrides, see: (*a*) M. C. Denney, N. A. Smythe, K. L. Cetto, R. A. Kemp and K. I. Goldberg, *J. Am. Chem. Soc.*, 2006, **128**, 2508; (*b*) G. R. Fulmer, R. P. Muller, R. A. Kemp and K. I. Goldberg, *J. Am. Chem. Soc.*, 2009, **131**, 1346; (*c*) R. Gerber, T. Fox and C. M. Frech, *Chem.–Eur. J.*, 2010, **16**, 6771; (*d*) C. Melero, L. M. Martínez-Prieto, P. Palma, D. Del Rio, E. Álvarez and J. Cámpora, *Chem. Commun.*, 2010, **46**, 8851.
10 For a dihydrogen complex of cobalt, see: T. J. Hebden, A. J. St. John, D. G. Gusev, W. Kaminsky, K. I. Goldberg and D. M. Heinekey, *Angew. Chem., Int. Ed.*, 2011, **50**, 1873.
11 (*a*) I. Göttker-Schnetmann, P. S. White and M. Brookhart, *Organometallics*, 2004, **23**, 1766; (*b*) V. Pandarus and D. Zargarian, *Organometallics*, 2007, **26**, 4321; (*c*) J. L. Bolliger, O. Blacque and C. M. Frech, *Chem.–Eur. J.*, 2008, **14**, 7969.
12 (*a*) K. Okamoto, T. Kanbara, T. Yamamoto and A. Wada, *Organometallics*, 2006, **25**, 4026; (*b*) K. Okamoto, T. Yamamoto, M. Akita, A. Wada and T. Kanbara, *Organometallics*, 2009, **28**, 3307; (*c*) J. Kuwabara, G. Munezawa, K. Okamoto and T. Kanbara, *Dalton Trans.*, 2010, **39**, 6255.
13 R. Gerber, O. Blacque and G. M. Frech, *ChemCatChem*, 2009, **1**, 393.
14 (*a*) C. Azerraf, A. Shpruhman and D. Gelman, *Chem. Commun.*, 2009, 466; (*b*) C. Azerraf, A. Shpruhman and D. Gelman, *Organometallics*, 2009, **28**, 6578.
15 (*a*) M. Gagliardo, N. Selander, N. C. Mehendale, G. van Koten, R. J. M. Gebbink and K. J. Szabó, *Chem.–Eur. J.*, 2008, **14**, 4800; (*b*) E. M. Schuster, M. Botoshansky and M. Gandelman, *Angew. Chem., Int. Ed.*, 2008, **47**, 4555; (*c*) E. M. Schuster, G. Nisnevich, M. Botoshansky and M. Gandelman, *Organometallics*, 2009, **28**, 5025; (*d*) E. M. Schuster, M. Botoshansky and M. Gandelman, *Organometallics*, 2009, **28**, 7001.
16 (*a*) H. M. Lee, J. Y. Zeng, C.-H. Hu and M.-T. Lee, *Inorg. Chem.*, 2004, **43**, 6822; (*b*) W. Weng, S. Parkin and O. V. Ozerov, *Organometallics*, 2006, **25**, 5345; (*c*) W. Weng, C.-H. Chen, B. M. Foxman and O. V. Ozerov, *Organometallics*, 2007, **26**, 3315.
17 (*a*) C. Freund, N. Barros, H. Gornitzka, B. Martin-Vaca, L. Maron and D. Bourissou, *Organometallics*, 2006, **25**, 4927; (*b*) P. Oulié, C. Freund, B. Martin-Vaca, L. Maron and D. Bourissou, *Organometallics*, 2007, **26**, 6793; (*c*) P. Oulié, N. Nebra, B. Martin-Vaca, L. Maron and D. Bourissou, *J. Am. Chem. Soc.*, 2009, **131**, 3493.
18 (*a*) S. Takahashi and M. Nonoyama, *Transition Met. Chem.*, 1995, **20**, 528; (*b*) D. E. Bergbreiter, P. L. Osburn and Y.-S. Liu, *J. Am. Chem. Soc.*, 1999, **121**, 9531; (*c*) D. R. Evans, M. Huang, W. M. Seganish, J. C. Fettinger and T. L. Williams, *Organometallics*, 2002, **21**, 893; (*d*) T. Kanaba and T. Yamamoto, *J. Organomet. Chem.*, 2003, **688**, 15; (*e*) M. A. Hossain, S. Lucarini, D. Powell and K. Bowman-James, *Inorg. Chem.*, 2004, **43**, 7275; (*f*) M. Akaiwa, T. Kanbara and T. Yamamoto, *J. Organomet. Chem.*, 2005, **690**, 4192; (*g*) R. A. Begum, D. Powell and K. Bowman-James, *Inorg. Chem.*, 2006, **45**, 964; (*h*) H. Meguro, T.-A. Koizumi, T. Yamamoto and T. Kanbara, *J. Organomet. Chem.*, 2008, **693**, 1109; (*i*) V. A. Kozlov, D. V. Aleksanyan, Y. V. Nelyubina, K. A. Lyssenko, E. I. Gustul, L. N. Puntus, A. A. Vasil'ev, P. V. Petrovskii and I. L. Odinets, *Organometallics*, 2008, **27**, 4062; (*j*) Y. Ogawa, A. Taketoshi, J. Kuwabara, K. Okamoto, T. Fukuda and T. Kanbara, *Chem. Lett.*, 2010, **39**, 385.
19 Similar ion pair association *via* N–H···Cl hydrogen bonding has been observed in $[Ph_3PN(Ph)H][PdCl_2(C_8H_{11})]$: D. Aguilar, F. Aznárez, R. Bielsa, L. R. Falvello, R. Navarro and E. P. Urriolabeitia, *Organometallics*, 2007, **26**, 6397.
20 For other examples of anionic Pd and Ni pincer complexes characterized by X-ray diffraction studies, see: D. Sellman, F. Geipel and F. Heinemann, *Eur. J. Inorg. Chem.*, 2000, 271.
21 For examples of anionic Pd pincer complexes too instable to be characterized structurally, see: (*a*) J. Liu, H. Wang, H. Zhang, X. Wu, H. Zhang, Y. Deng, Z. Yang and A. Lei, *Chem.–Eur. J.*, 2009, **15**, 4437; (*b*) M. Feller, E. Ben-Ari, M. A. Iron, Y. Diskin-Posner, G. Leitus, L. J. W. Shimon and L. Konstantinovski, *Inorg. Chem.*, 2010, **49**, 1615.
22 The NMR spectra showed only one set of signals, denoting that only one isomer was also present in solution.
23 M. Noskowska, E. Sliwinska and W. Duczmal, *Transition Met. Chem.*, 2003, **28**, 756.
24 K. A. Falls, G. K. Anderson and N. P. Rath, *Organometallics*, 1992, **11**, 885.
25 M. Stradiotto, C. M. Kozak and M. J. McGlinchey, *J. Organomet. Chem.*, 1998, **564**, 101.
26 Atom numbering for the NMR assignments:.

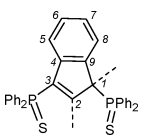

27 *Nuclear Magnetic Resonance Spectroscopy*, F. A. Bovey, Ed., Academic Press, New-York, 1969; R. J. Abraham and H. Berstein, *Can. J. Chem.*, 1961, **39**, 216.
28 *SADABS, Program for data correction*, Bruker-AXS, 2003, version 2.10.
29 G. M. Sheldrick, *SHELXL-97, Program for refinement of crystal structures*, University of Göttingen, Germany, 1997.

30 G. M. Sheldrick, *Acta Crystallogr., Sect. A: Found. Crystallogr.*, 1990, **46**, 467.
31 D. Andrae, U. Haeussermann, M. Dolg, H. Stoll and H. Preuss, *Theor. Chim. Acta*, 1990, **77**, 123.
32 A. Bergner, M. Dolg, W. Kuechle, H. Stoll and H. Preuss, *Mol. Phys.*, 1993, **80**, 1431.
33 A. W. Ehlers, M. Böhme, S. Dapprich, A. Gobbi, A. Höllwarth, V. Jonas, K. F. Köhler, R. Stegmann, A. Veldkamp and G. Frenking, *Chem. Phys. Lett.*, 1993, **208**, 111.
34 P. C. Hariharan and J. A. Pople, *Theor. Chim. Acta*, 1973, **28**, 213.
35 A. D. Becke, *J. Chem. Phys.*, 1993, **98**, 5648.
36 K. Burke, J. P. Perdew, W. Yang, *Electronic Density Functional Theory: Recent Progress and New Directions*, J. F. Dobson, G. Vignale and M. P. Das, Ed., Springer, Heildelberg, 1998.
37 M. J. Frisch, G. W. Trucks, H. B. Schlegel, G. E. Scuseria, M. A. Robb, J. R. Cheeseman, J. A. Montgomery, Jr., T. Vreven, K. N. Kudin, J. C. Burant, J. M. Millam, S. S. Iyengar, J. Tomasi, V. Barone, B. Mennucci, M. Cossi, G. Scalmani, N. Rega, G. A. Petersson, H. Nakatsuji, M. Hada, M. Ehara, K. Toyota, R. Fukuda, J. Hasegawa, M. Ishida, T. Nakajima, Y. Honda, O. Kitao, H. Nakai, M. Klene, X. Li, J. E. Knox, H. P. Hratchian, J. B. Cross, V. Bakken, C. Adamo, J. Jaramillo, R. Gomperts, R. E. Stratmann, O. Yazyev, A. J. Austin, R. Cammi, C. Pomelli, J. Ochterski, P. Y. Ayala, K. Morokuma, G. A. Voth, P. Salvador, J. J. Dannenberg, V. G. Zakrzewski, S. Dapprich, A. D. Daniels, M. C. Strain, O. Farkas, D. K. Malick, A. D. Rabuck, K. Raghavachari, J. B. Foresman, J. V. Ortiz, Q. Cui, A. G. Baboul, S. Clifford, J. Cioslowski, B. B. Stefanov, G. Liu, A. Liashenko, P. Piskorz, I. Komaromi, R. L. Martin, D. J. Fox, T. Keith, M. A. Al-Laham, C. Y. Peng, A. Nanayakkara, M. Challacombe, P. M. W. Gill, B. G. Johnson, W. Chen, M. W. Wong, C. Gonzalez and J. A. Pople, *GAUSSIAN 03 (Revision D.02)*, Gaussian, Inc., Wallingford, CT, 2004.
38 A. E. Reed, L. A. Curtiss and F. Weinhold, *Chem. Rev.*, 1988, **88**, 899.